technical notes Journal of proteome research

Quantitative Analysis of HGF and EGF-Dependent Phosphotyrosine Signaling Networks

Dean E. Hammond,[†] Russell Hyde,[†] Irina Kratchmarova,[‡] Robert J. Beynon,[†] Blagoy Blagoev,*[,‡] and Michael J. Clague*[,†]

Physiological Laboratory, School of Biomedical Sciences, University of Liverpool, Crown Street, Liverpool, L69 3BX, United Kingdom, and Department of Biochemistry and Molecular Biology, Center for Experimental BioInformatics, University of Southern Denmark, 5230 Odense, Denmark

Received July 12, 2009

Abstract: We have used stable isotope labeling by amino acids in cell culture (SILAC), in combination with high-resolution mass spectrometry, to identify common and discrete components of the respective receptor tyrosine kinase-dependent phosphotyrosine-associated networks induced by acute stimulation of A549 lung adenocarcinoma cells with EGF or HGF. In total, we obtained quantitative information for 274 proteins, which respond to either or both stimuli by >1.5 fold changes in enrichment, following immuno-precipitation with antiphosphotyrosine antibodies. The data reveal a high degree of overlap between the respective signaling networks but also clear points of departure. A small number of HGF specific effectors were identified including myosin-X, galectin-1, ELMO2 and EphrinB1, while a larger set of EGF specific effectors (39 proteins) includes both novel (e.g., MAP4K3) and established components of receptor tyrosine kinase receptor signaling pathways. Using available protein-interaction data the identified proteins have been assembled into a highly connected network that can be visualized using the Cytoscape tool.

Keywords: HGF • EGF • SILAC • receptor tyrosine kinase • Met receptor

Introduction

The human genome contains 59 receptor tyrosine kinases (RTKs), which show widely varying expression profiles congruent with the control of differing physiological outputs.[1] In all cases, acute stimulation elicits a complex signaling network triggered by the action of the receptor kinase activity. Recent developments in quantitative mass spectrometry have opened new avenues for the analysis of such complex cellular signaling pathways. Among many other applications, stable isotope labelling by amino acids in cell culture (SILAC) combined with mass spectrometry has been used to analyze RTK signaling networks,[2−7] following immunoprecipitation with antiphosphotyrosine (pTyr) antibodies. RTK signaling networks, which have been studied in this way, include the EGF receptor (EGFR),[7] Her2/neu receptor,[8] Insulin receptor,[5] and the PDGF receptor (PDGFR).[6]

It is known that stimulation of different RTKs in the same cell line can mediate both common and distinct cellular behaviors. It is an important issue in signal transduction research as to the degree to which these signaling networks overlap. There are still few global comparisons of RTK signaling networks. The identification of factors specific to a given stimulus is not presently possible by comparison of isolated data sets but can be accomplished by direct comparison in the same quantitative proteomic experiment. An outstanding example of this approach is the analysis of PDGFR- and EGFR-dependent signaling in human mesenchymal stem cells, which led to the identification of the class I PtdIns 3-kinase pathway specific to PDGF signaling, as a suppressor of differentiation into osteoblasts.[6] In this study we have applied a similar approach to directly compare HGF signaling through the Met receptor with EGF receptor activation in A549 lung carcinoma cells. The receptors are proposed to diversify signal outputs through different means. For Met, phosphorylation of Tyr^{1349} and Tyr^{1356} generates a multisubstrate docking site[9] in contrast with seven pTyr residues that serve as docking sites on the EGFR. Hence Gab1 adaptor protein plays a critical role in diversifying HGF-signaling outputs.[10]

Met receptor expression is largely confined to cells of epithelial origin, where it controls a complex genetic program leading to so-called invasive growth.[11,12] Aberrant HGF-Met signaling is widely implicated in the generation and spread of tumors and metastases and has also been implicated in the acquisition of resistance to Gefitinib in cells with activating EGFR mutations.[13,14] A recent study has compared the activation of pTyr signaling in cells transformed by oncogenic EGFR and over-expressed Met receptors respectively.[15] The present study provides complementary information on the response of a single cell line to an acute stimulation with either HGF or EGF, enabling a more direct comparison. Our data set uncovers several new EGF effectors, but as importantly provides the first comprehensive analysis of HGF-dependent signaling and the identification of several factors specific to HGF stimulation. Furthermore, pharmacological inhibition of Met can render EGFR mutant nonsmall cell lung cancer cell lines sensitive to EGFR inhibitors.[13,14] Thus, the identification of common downstream signaling nodes in A549 lung adenocarcinoma

* To whom correspondence should be addressed. E-mail: clague@liv.ac.uk, bab@bmb.sdu.dk.
[†] University of Liverpool.
[‡] University of Southern Denmark.

10.1021/pr100145w

Published on Web 03/11/2010

cells may provide an inventory of potential points of alternate pharmacological intervention.

Materials and Methods

Cell Culture and SILAC. The SILAC cell culture medium, Dulbecco's Modified Eagles Medium (DMEM) deficient in arginine, lysine and leucine, was a custom preparation from Invitrogen. L-Arginine U−^{13}C6 ($^{13}C_6{}^{14}N_4$−Arg) and L-Arginine U−$^{13}C_6{}^{15}N_4$ ($^{13}C_6{}^{15}N_4$−Arg) were obtained from Cambridge Isotope Laboratories. Dialyzed fetal bovine serum (FBS) was added to 10% (v/v). A549 cells were labeled to equilibrium over 21 days. Cells were serum starved for 16 h prior to stimulation with 100 ng/mL EGF or HGF for 5 or 30 min.

Antibodies and Immunoprecipitation. Antibodies against the following proteins were used: for immunoprecipitation, immobilized anti-pTyr antibodies (4G10 (Millipore) and P-Tyr-100 (Cell Signaling)); for Western blot analysis, Met, EGFR, CBL, Dab2 and ERK-1 (Santa Cruz), PI3KC2α and PI3KC2β (BD Transduction Laboratories), MIG6, GAB1, GAB2 and GRB2 (Cell Signaling), HRS (Axxora), MAP4K3 (gift of R. Lamb, Institute of Cancer Research, London, UK) and SNX9 (gift of S. Schmid, Scripps Research Institute, La Jolla, California). pTyr immunoprecipitation was performed as described in ref 7.

Two experimental configurations/lysate mixtures were used: unstimulated (Arg-0), 5 min EGF (Arg-6) and 5 min HGF (Arg-10); and, unstimulated (Arg-0), 30 min EGF (Arg-10) and 30 min HGF (Arg-6). Lysates encompassing each set of three conditions were pooled precleared on Protein A (extracellular) agarose beads for 1 h at 4 °C to reduce nonspecific binding of abundant cellular proteins, then separated from the Protein A beads following centrifugation and transferred to fresh tubes. Each mixture was then incubated with 1 mg agarose-conjugated anti-pTyr antibody 4G10 for 2 h followed by an additional 4 h incubation with 400 μL anti-pTyr P-Tyr-100. Immunoprecipitated complexes were then washed three times with approximately 25 volumes of lysis buffer (plus phosphatase inhibitors) and then eluted with glycine pH 2.5. The eluates were concentrated initially on Centricon spin columns (10 kDa cut off; Millipore) and subsequent vacuum centrifugation, after which they were neutralized with a buffer containing 2 M Tris (pH 8), 1.5 M NaCl, and 1 mM EDTA, mixed with SDS sample buffer, and separated on a NuPAGE Novex 4−12% Bis-Tris gel (InVitrogen).

For the Western blotting experiments scaled down immunprecipitations were performed and proteins were electrotransferred onto nitrocellulose membrane, blocked and then probed with the corresponding primary antibodies, followed by IR dye-coupled secondary antibodies, detected using the Odyssey system (LI-COR).

Mass Spectrometric Analysis, Peak List Generation, Database Searching, and Validation. After SDS-PAGE and peptide extraction[16] samples were processed for liquid chromatography−mass spectrometry (LC−MS). Reverse phase nano-LC was performed on an Agilent 1100 nanoflow LC system (Agilent Technologies). The LC system was coupled to a 7-T LTQ-FT instrument (Thermo Fisher Scientific) equipped with a nanoeletrospray source (Proxeon). The peak list files were searched against a concatenated decoy IPI-human database (version 3.57) containing both forward and reversed protein sequences, by the MASCOT search engine (version 2.2.04, Matrix Science[17]). The raw files were processed with the MaxQuant software suite (version 1.0.12.31) which offers statistically robust identification and quantitation.[18]

The minimum required peptide length was set to 6 amino acids and two missed cleavages were allowed. Cysteine carbamidomethylation (C) was set as a fixed modification, whereas oxidation (M), S/T phosphorylation, Y phosphorylation, N-terminal protein acetylation, and deamidated (NQ) were considered as variable modifications. The initial precursor and fragment ion maximum mass deviations in the database search were set to 7 ppm and 0.5 Da, respectively, which is optimal for linear ion trap data.[19] The results of the database search were further processed and statistically evaluated within MaxQuant. The false discovery rate (FDR) for both the peptides and proteins were set to 0.01 to ensure that the worst identified peptide/protein has a 1% probability of being a false identification. Proteins with at least two peptides (with one unique to the protein sequence) were considered as valid identifications.

For identification of pTyr-containing peptides, the raw data files were processed with MaxQuant (version 1.0.13.13). Assignment of the phosphorylated Tyr residue within any identified phosphopeptides was based on the localization post-translational modification (PTM) scoring algorithm as previously described.[20] To determine whether any identified phosphopeptides were novel, the phosphorylated Tyr residue(s) assigned were searched against the phosida (www.phosida.de) and PhoshpoELM (http://phospho.elm.eu.org) databases.

Protein Interaction Data/Visualization. Human protein−protein interaction data were obtained from HPRD (release 7; www.hprd.org), NetPATH (dated 1/4/08; http://www.netpath.org/), BioGRID (version 2.0.45; www.thebiogrid.org), MINT (dated 8/4/08; http://mint.bio.uniroma2.it/mint/Welcome.do) and IntAct (dated 8/10/08; http://www.ebi.ac.uk/intact/site/index.jsf). Gene identifiers within the data were converted to NCBI-Entrez format for consistency and the interaction data were imported into R v2.7.0/Bioconductor v2.2 for analysis (http://www.r-project.org/; http://www.bioconductor.org/) and Cytoscape v2.6.2 for visualization (http://www.cytoscape.org/).

The complete human interaction network comprised 10702 proteins and 55555 interactions. From this data set, a subnetwork containing the EGF and/or HGF responsive proteins was generated. To study this network: (a) download Cytoscape from the link above (use version 2.6.2 if the most recent version causes any problems); (b) copy/open the text from the excel files Hammond et al.xls and Hammond et al_props.xls into a text editor and save the files as Hammond et al.xgmml and Hammond et al.props respectively; (c) import the .xgmml file from the Supporting Information into Cytoscape (using 'File→Import→Network,multiple file types'); (d) import the visual style .props file from the Supporting Information (using 'File→Import→Vizmap property file') and set the current visual style to 'MAVals_5 min' (using 'View→Open Vizmapper' and then selecting the option 'MAVals_5 min' from the drop-list under 'Current Visual Style'). The image on screen should be identical to that in Figure 4. For each node in the network, the following calculations were performed:

$$M = \log_2(\mathrm{EGF}/\mathrm{HGF})$$

$$A = \log_2((\mathrm{EGF} \times \mathrm{HGF})^{1/2})$$

The values EGF and HGF are the fold change in protein abundance in the pTyr-immunoprecipitate following treatment with the corresponding growth factor.

Results

Immunoprecipitation conditions were achieved that allowed high coverage of the pTyr-associated proteome by mass spectrometry. Our full data set contains 274 proteins that were quantifiable using MaxQuant software and which exhibit ≥1.5 fold change in efficiency of immunoprecipitation with anti-pTyr antibodies following stimulation with either EGF or HGF (Supplementary Table 1, Supporting Information). Peptides corresponding to EGFR (80) and Met receptor (60) were detected at similar abundance. Peptide mass spectra representative of proteins enriched by stimulation with either (or both) growth factor are shown in Figure 1, together with a general schematic diagram of the adopted experimental procedure. Out of these 274 proteins, 226 exhibit ≥1.5 fold change in enrichment following EGF stimulation after either (or both) 5 and 30 min stimulation (163/274 proteins ↑, 73/226 proteins ↓). 214 proteins show ≥1.5 change following either 5 or 30 min HGF stimulation (140/214 proteins ↑, 82/214 proteins ↓). We confirmed enrichment of selected quantitated proteins showing ≥1.5 fold change using Western blotting (Figure 2). We used the post-translational modification (PTM) scoring algorithm inbuilt within MaxQuant (version 1.0.13.13) to unequivocally detect and map phosphotyrosine modified peptides, in this case, from 52 proteins (Supplementary Table 2, Supporting Information).

Several previous studies have identified effectors of EGF signaling using SILAC or ICAT,[3,6,7,21−23] collectively yielding 222 proteins of interest. We find 56 of these among our set of 274 quantitated proteins (25% coverage). The studies which most closely resemble our own in experimental design,[3,6] albeit with different cell types, identified 130 unique EGF-responsive proteins, with 52 proteins common to both studies. We identify 46 of these proteins (35.4% coverage). Another study has identified phosphopeptides in nonsmall cell lung carcinoma cells driven by mutant EGFR and gastric cancer cells driven by overexpressed Met.[15] Our data set contains 15 of the 30 proteins they identified to be sensitive to inhibitors of receptor tyrosine kinase activity. In total, we identified 83 nonredundant pTyr phospho-sites from 52 phosphoproteins, of which Guo et al. see 33.[15] We detect 19 phosphorylated Tyr residues not previously reported in the literature (Supplementary Table 1 and 2, Supporting Information).

High Stringency EGF-Specific Effectors. In addition to the EGF receptor itself, 39 proteins were classified as highly biased toward EGF stimulation, showing either no substantive change following HGF, or ≥2 fold enrichment for EGF over HGF stimulation (Table 1). Of these, 33 were also quantitated at 30 min and, with some exceptions (e.g., ANKRD13A, PTPN23, α-actinin-4, SHC-1, VAV2), exhibit a general trend toward partial attenuation. Known specific interactors with the EGFR such as ErbB2 receptor[24] and MIG6/RALT[25,26] are found within this list, but the majority have either not previously been associated with EGFR signaling (e.g., MAP4K3) or were not thought to harbor specificity for EGFR over Met signaling (e.g., SOS1).

Specific and Highly Favored HGF Effectors. Far fewer proteins indicate stringency for HGF signaling (Table 1). We reason that this reflects the fact that nearly all Met signal diversification is mediated through the adaptor proteins Gab1 and Gab2, which can also be recruited by activated EGF receptor. Of these proteins, several have intriguing functions congruent with Met function. Myosin-X is a molecular motor which is involved in filopodium formation.[27] The membrane

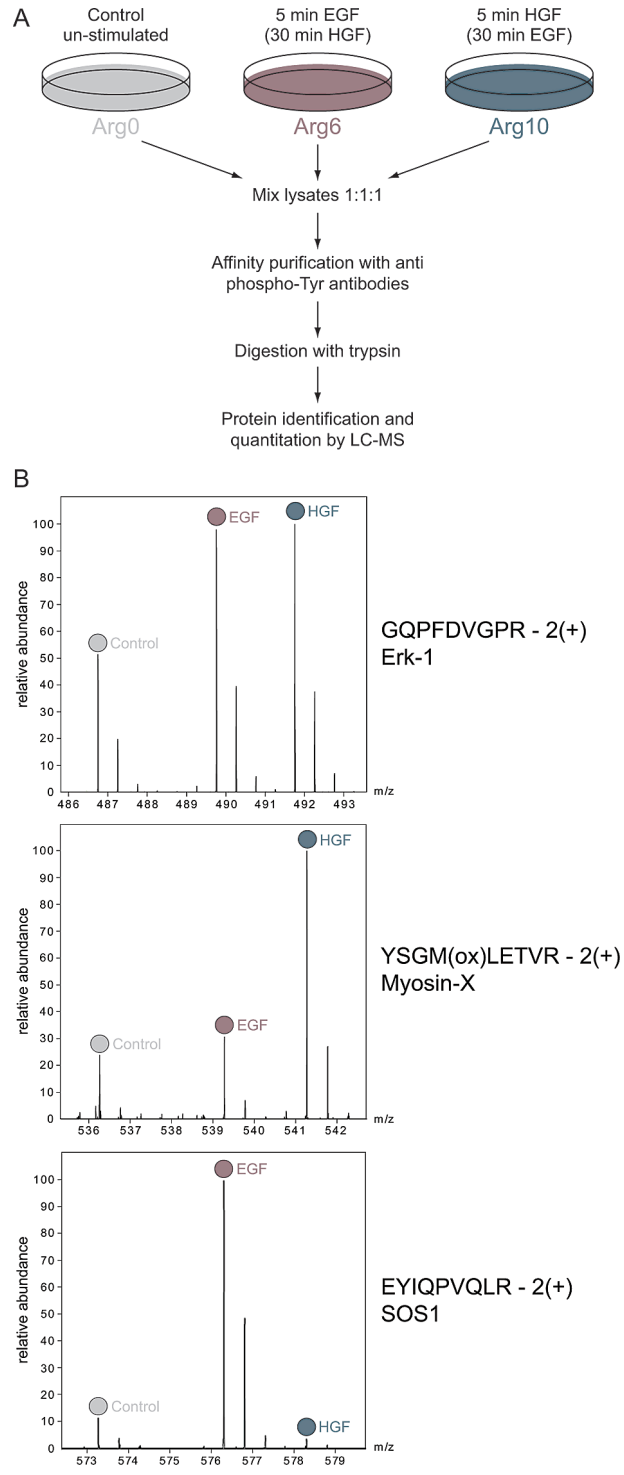

Figure 1. Schematic diagram of experimental procedure and representative mass spectra. (A) SILAC labeling configuration and applied stimuli. (B) MS/MS spectra of tryptic peptides derived from Erk-1 (top) shows a similar response to HGF or EGF while peptides from Myosin-X (middle) and SOS1 (bottom) show highly biased responses to HGF or EGF, respectively.

associated protein galectin-1 and Engulfment and cell motility 2 (ELMO2) have suggested roles in tumor invasion and migration.[28,29] The Abeleson famly of tyrosine kinases (here represented by ABL2) have an established role in regulating the actin cytoskeleton.[30] Ephrin B1 is a type 1 membrane protein and ligand for Eph-related receptor kinases, which may

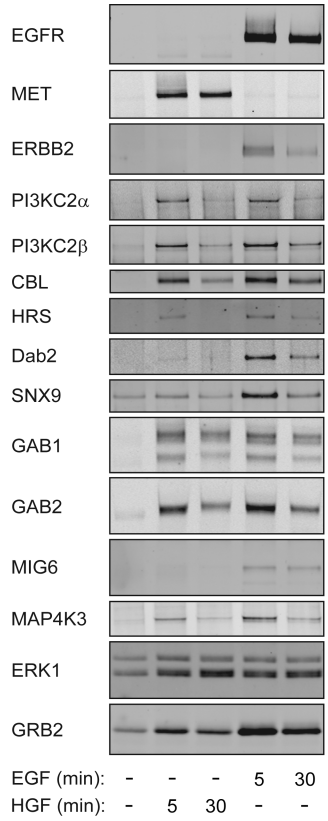

Figure 2. Western blot analysis of enrichment for selected proteins. A549 cells were stimulated for 5 and 30 min with growth factors and immunoprecipitated with anti-pTyr antibodies.

play a role in cell adhesion.[31] Notably we do not find specific enrichment of various cell-surface adhesion molecules which have been suggested to be cofactors in Met signaling.[32,33]

Network Properties. We have analyzed the frequency of particular protein domains germane to RTK signaling, within our set of 274 proteins (Figure 3). As expected, proteins containing SH2 and SH3 domains are strongly represented, but ubiquitin and lipid binding domains are also prominent. In order to visualize protein interaction information within our data set, a subnetwork containing EGF and/or HGF responsive proteins was produced from an in-house generated complete human interaction network, comprising of 10702 proteins and 55 555 interactions. The EGF/HGF network contained 273 proteins (2 proteins could not be given a unique entrez ID). 168/273 proteins were present in a large connected network (Figure 4), which can be viewed using Cytoscape[34] by loading the files provided in Supporting Information and following instructions described in materials and methods. 83 proteins were found which have interaction partners in the human interaction network but do not link directly link into the 168 protein cluster. In addition, 22 proteins in the list do not currently have any documented interaction partners (square nodes in Figure 4). 172 proteins have known interaction partners among the 274 proteins and 143 (83%) of these are within 2 degrees of separation from one or both receptors (Figure 4). Met receptor is known to interact directly with 12 other proteins in the network, excluding EGFR. All of these also interact directly with EGFR and are over-represented by highly connected "hub" proteins (median number of interactions within the network = 21), expanding the network to 115 s degree interactions with the Met receptor. Of the 47 remaining proteins which interact directly with EGFR, the median number of interactors is 6. 251/274 have known interaction partners within the total protein interaction database. The network contains 602 interactions, compared with an average of 84 for 251 proteins selected at random from the interaction database. The distribution of degree of interactions is clearly skewed from randomly generated sets (Supplementary Figure 1, Supporting Information).

Discussion

The 274 quantitated proteins are listed in full in Supplementary Table 1 (Supporting Information). Here we provide a breakdown by association with major signaling functions:

Lipid and Protein Kinases. Previous comparison of PDGF and EGF signaling highlighted functionally significant differences in signaling through class I PtdIns 3-kinases, which generate the signaling lipid PtdIns(3,4,5)P_3.[6] In this study, we identify more prominent enrichment of both class II PtdIns 3-kinase isoforms PI3KC2α and PI3KC2β, consistent with results of Arcaro et al. using immunoprecipitation of activated EGFR.[35] The involvement of these lipid kinases in cell signaling pathways is only just beginning to be unravelled. PI3KC2α and PI3KC2β have been shown to generate PtdIns3P in response to insulin and lysophosphatidic acid stimulation respectively.[36,37]

MAP4K3 has not been previously linked to EGF signaling but is highly enriched following EGF stimulation. It is proposed to bind endophilin, to regulate c-Jun N-terminal kinase (JNK)[38] and to act as nutrient sensitive regulator of mTOR signaling.[39] Other prominent kinases enriched by both stimuli including p38 MAP kinase/MAPK14, ERK-2/MAPK1, ERK-1/MAPK3. BMK1/MAPK7 were only detected at the 30 min time-point.

Phosphatases. Among phosphatases, the inositol 5-phosphatase SHIP-2 and PTPN23/HD-PTP show specificity for EGF over HGF stimulation, as well as the histidine phosphatase family member Suppressor of T-cell receptor signaling 1 (Sts-1), which has been shown to dephosphorylate EGFR directly.[40,41] Others showing pronounced enrichment with both stimuli include PTPN11/SHP2, and acid phosphatase 1/low molecular weight phosphatase (ACP1α/LMW-PTP). PTPN11 is a proto-oncogene, for which germ-line gain of function mutations lead to Noonan's syndrome.[42]

GTPase Signaling. Small GTPases play key roles in growth factor signaling, although they are rarely tyrosine phosphorylated directly. Instead, accessory molecules such as nucleotide exchange factors and GTPase activating proteins (GAPs) may be recruited to phosphorylated residues. The ras and rac exchange factors SOS-1, Vav-2, and Vav-3 are specifically enriched in the EGF network. The rab5 exchange factor RIN1 show a more complex pattern of enrichment by HGF at 5 min, but EGF-dependent enrichment exclusively at 30 min. De-enrichment is fairly common among GTPase regulators following HGF or EGF. Clear examples include rhoGAP10, CDC42 GAP, and the ras associating protein RASSF7.

Two small GTPases, rab7 and rab11, both associated with the endocytic pathway are directly enriched. Also noteworthy is our identification of two members of the septin family of GTPases (septins 2 and 9). Best known for control of cytokinesis, members of this family have recently been implicated in regulation of membrane trafficking processes.[43,44]

Ubiquitin Modifiers. There is increasing appreciation that ubiquitination represents a reversible modification which not only specifies degradation, but is actively involved in signal transduction. Significant cross-talk occurs between ubiquitin

Table 1. Selected Proteins and Their Response to Growth Factor Stimuli[a]

		ratio after growth factor stimulation			
		EGF		HGF	
Uniprot ID	protein name	5 min	30 min	5 min	30 min
	Highly enriched after EGF-stimulation				
P00533	EGFR	29.8	23.2	0.9	0.8
Q8IZ07	ANKRD13A	5.8	15.8	0.7	1.1
Q9UJM3	MIG6/RALT	13.6	4.4	1.6	0.9
Q15417	Calponin-3	6.5	1.1	0.9	1.0
Q92734	TFG	9.8	0.1	1.6	0.7
Q8IVM0	Ymer	11.4	1.8	2.0	0.6
P04626	ErbB-2	5.7	2.5	1.2	0.6
Q8IVH8	MAP4K3	13.6	–	3.1	–
Q9Y5A9	YTH domain family protein 2	10.6	–	2.4	–
P98082	DAB2	40.2	–	9.4	–
A8K5U9	PICALM	17.9	1.9	4.3	1.7
Q07889	SOS1	5.6	2.6	1.3	0.6
Q9BYM8	RNF54	2.9	1.0	0.7	0.5
O00750	PI3K C2β	14.3	5.0	3.6	1.0
P50995	Annexin A11	8.8	2.5	2.2	1.4
O15357	SHIP-2	9.2	8.1	2.5	1.9
P63010	AP-2 β−1	–	3.4	–	0.9
P35609	α-actinin-2	3.6	–	1.1	–
O43707	α-actinin-4	1.3	2.4	0.9	1.0
Q93008	USP9X	5.1	2.0	1.6	1.1
Q92738	USP6 N-terminal-like/RN-tre	3.3	1.6	1.0	1.7
Q15365	Poly(rC)-binding protein 1	2.6	1.8	0.8	1.0
Q8TF42	STS-1	4.9	2.0	1.8	1.1
B5BU19	SHC-1 (Isoform 3)	4.0	8.4	1.9	2.4
Q92783	STAM1	18.2	10.5	9.0	2.3
P52735	VAV2	2.1	4.2	1.3	0.9
Q9UKW4	VAV3	2.0	0.6	1.2	1.0
O14492	SH2B2	2.6	–	1.3	–
Q05209	PTPN12	2.2	1.3	1.1	0.9
Q9H3S7	PTPN23	6.7	8.2	4.2	1.8
A7KAX9	Rho/Cdc42/Rac GAP RICS	1.9	1.1	0.9	1.1
P15311	Ezrin	1.8	1.2	1.0	0.9
P35221	Catenin α−1	1.8	1.1	1.1	0.7
O60716	Catenin δ−1	1.6	1.0	1.0	0.7
P61978	hnRNP K	2.7	1.6	1.1	1.0
Q68CZ2	Tensin-3	2.2	1.3	1.0	1.1
A6NMJ7	Tensin-4	1.6	0.6	0.8	0.7
Q9Y3I0	UPF0027 protein C22orf28	2.0	1.3	1.1	1.0
A7E2F8	Tankyrase 1-binding protein 1	2.7	2.7	1.3	1.0
Q9UII7	E-cadherin	2.6	1.0	1.2	0.5
	Enriched after HGF-stimulation				
A0PJF7	MET Receptor	0.8	0.8	27.0	9.2
Q86YZ3	Hornerin	–	0.4	–	3.0
P42684	ABL2	1.8	–	4.3	0.5
Q96JJ3	ELMO2	1.0	–	3.6	–
P98172	Ephrin-B1	0.9	–	3.4	–
Q00610	Clathrin HC 1	2.3	2.1	6.1	3.5
Q9HD67	Myosin-X	1.3	0.9	3.5	0.5
Q3KQZ2	SYNGR2 protein	2.5	–	6.7	–
Q9H6X2	Anthrax toxin receptor 1	1.1	1.2	2.2	1.1
P09382	Galectin-1	–	1.1	–	1.8
Proteins with increased abundance (≥1.5-fold) after either or both EGF or HGF					
Kinases and phosphatases					
P37173	TGF-βR (type-2)	1.4	1.1	1.6	1.0
P28482	MAPK 1/ERK-2	2.9	2.4	2.7	2.3
P27361	MAPK 3/ERK-1	2.4	1.8	2.3	1.7
B4DI23	MAPK 7/ERK-5	–	5.3	–	6.0
Q16539	MAPK 14/p38α MAPK	4.0	–	4.7	–
O00443	PI3K C2α	9.6	–	7.6	–
P42338	p110 PI3Kβ	1.6	1.9	2.2	2.1
P27986	p85 PI3Kα	2.2	1.4	2.3	1.5

Table 1. Continued

		ratio after growth factor stimulation			
		EGF		HGF	
Uniprot ID	protein name	5 min	30 min	5 min	30 min
O00459	p85 PI3Kβ	2.1	2.1	2.9	2.7
P30530	AXL/UFO	1.8	1.7	1.6	1.8
P06493	CDC2	1.1	1.9	1.1	1.9
P24941	CDK2	1.3	2.2	1.2	2.4
Q14289	PTK2β	1.3	1.4	1.0	1.7
B4DL04	Ephrin receptor EphA2	1.4	1.6	1.2	0.9
P78527	DNA-dependent protein kinase	2.0	–	1.3	–
Q07912	Activated CDC42 kinase 1	6.5	–	3.2	–
P08069	Insulin-like GF 1 receptor	–	2.2	–	3.1
Q06124	PTPN11/SHP-2	7.4	4.5	9.8	5.7
P24666	ACP1α	2.6	1.5	3.7	0.5
	Ubiquitin related				
A3KMP8	CBL	37.0	14.8	37.3	5.4
Q13191	CBL-B	15.7	6.4	9.3	3.2
Q8NC42	RNF149	1.5	1.0	1.8	0.9
Q9BT67	NEDD4 family interacting protein 1	1.4	1.0	1.6	0.9
Q9NQC7	CYLD	1.6	–	1.3	–
A8K674	Ubiquitin C	5.1	3.6	2.7	1.4
	Endocytic proteins				
Q9H0E2	TOLLIP	2.1	1.1	1.4	0.8
O75674	TOM1-like 1	2.2	1.0	1.2	0.9
Q6ZVM7	TOM1-like 2	3.3	2.4	5.5	1.9
O14964	HRS/HGS	12.9	8.7	11.0	5.1
O95208	Epsin-2	5.3	–	9.9	–
Q9NZM3	Intersectin 2	3.9	1.0	5.1	2.1
Q5VWQ8	DAB2-IP	1.6	1.4	1.4	1.8
P42566	Eps15	19.1	4.2	19.6	2.5
A2RRF3	Eps15-like 1	3.4	1.5	5.6	1.8
Q8WUM4	PDCD6-IP	2.0	1.1	1.5	0.8
Q9Y5X1	SNX9	2.0	–	–	–
Q9NZN4	EH domain-containing protein 2	–	11.9	–	9.6
Q7Z3T8	Endofin	21.3	–	7.3	–
Q96QK1	VPS35	1.3	1.0	1.5	1.5
	Adaptor proteins/signaling scaffolds				
Q13480	GAB1	11.7	6.3	13.0	7.5
Q9UQC2	GAB2	14.6	4.0	7.2	3.5
P62993	GRB2	2.2	2.1	1.3	1.3
P29353	SHC-1 (Isoform p66Shc)	7.3	0.9	2.8	1.4
Q9NZQ3	SPIN90	6.9	2.2	4.0	2.4
Q9Y2A7	Nck-associated protein 1	1.9	1.4	3.1	1.6
Q14847	LASP1	2.5	1.6	1.6	1.3
Q15464	SHB	1.9	2.1	0.9	1.3
Q15464	SHB (Isoform 2)	–	2.0	–	1.2
Q9C0H9	p130Cas-associated protein	0.8	1.8	0.8	1.7
Q15750	MAPKKK 7-interacting protein 1	9.7	–	3.7	–

[a] Highly specific EGF-enriched proteins show an enrichment of ≥2 and either do not respond to HGF or show an enrichment ratio of EGF/HGF > 2.5.

and phosphorylation events.[45] The E3-ubiquitin ligase c-Cbl promotes the lysosomal degradation of both EGFR[46] and Met.[47] Accordingly, we find abundant peptides derived from c-Cbl and its paralogue Cbl-B highly enriched following either stimulus. Several other ubiquitin modifying proteins are enriched. The E3-ligase, RanBP-type and C3HC4-type zinc finger-containing protein 1/RNF54/UCE7-IP3 is intimately connected with the EGF-signaling pathway where it may act to ubiquitinate substrates. The deubiquitinating enzyme (DUBs) USP6 and USP9X, are specifically enriched following EGF stimulation. USP6/TRE17 has been suggested to be in complex with CDC42 and rac1 regulating actin rearrangements.[48] Its knock-down also leads to decreased activation of arf6, a GTPase associated with cell invasion.[49] USP9X has been shown to regulate the ubiquitin status of epsin[50] and of AMPK-related kinase.[51]

Concluding Remarks. The introduction of large-scale proteomic approaches to study signaling networks has revealed the complexity of the network response to RTK activation. Future work can examine contingencies within these networks through pharmacological intervention upon specific nodes or by their specific knock-down. This work significantly expands the repertoire of proteins associated with EGFR activation and provides the first large-scale study associated with acute Met receptor activation. By comparing receptors, we can see a high degree of overlap between the signaling networks, consistent with shared phenotypic outcomes such as cell proliferation or

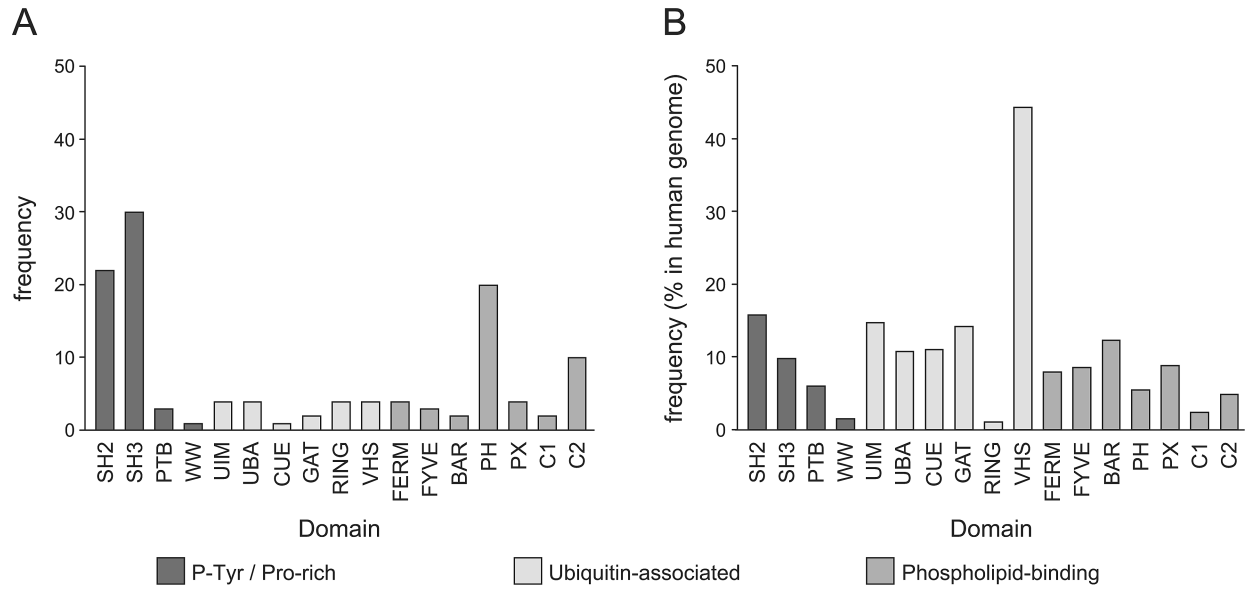

Figure 3. Incidence of common signaling domains. (A) Frequency of proteins containing designated domains within the quantitated data set of 274 proteins. (B) Frequency of these domains normalized to the number of each domain found in the human genome.

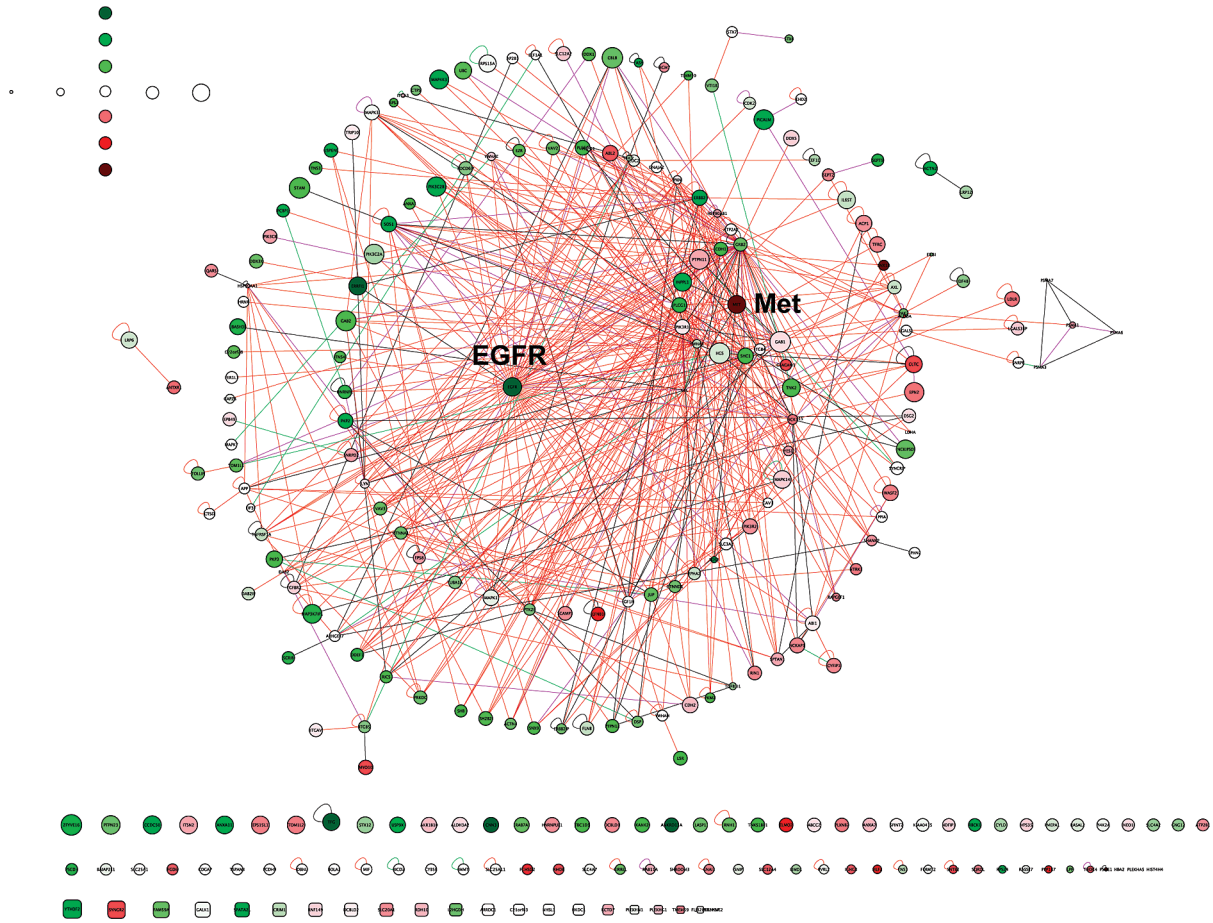

Figure 4. EGF/HGF responsive proteins form a highly connected network. EGF and/or HGF responsive proteins and known interactions within this set are shown as nodes and edges, respectively. Interactions were mined from several databases (see Methods). The inner circle represents first degree interactions with EGFR or with both Met and EGFR (12 indented nodes). Node size reflects the geometric mean of the 5 min EGF and HGF responses; node color reflects the EGF:HGF response ratio at 5 min (green, increase with EGF > HGF; red, increase with HGF > EGF; conversely for decreases). Red edges correspond to interactions from yeast two hybrid (Y2H) studies; purple, Y2H + interlog; green, other methods. The protein interaction network generated is included as Supporting Information. Instructions for opening within the network visualization tool Cytoscape are provided in Methods. Cytoscape allows for manipulation of the network and visualization of node attributes.

scattering. By illustrating this high degree of overlap in pTyr signaling networks, our data help us understand why EGFR mutant transformed cells may respond to gefitinib treatment by amplification of Met.[13] While therapies involving combinations of RTK kinase inhibitors are being considered, studies such as ours can also inform on potential downstream targets common to receptors.

Acknowledgment. This work was supported by Cancer Research U.K. I.K. and B.B. were supported by the Danish Natural Science Research Council. We thank Mary Doherty for initial help with MS and Sylvie Urbé for helpful discussion.

Supporting Information Available: Supplemental Figures and Tables. This material is available free of charge via the Internet at http://pubs.acs.org.

References

(1) Manning, G.; Whyte, D. B.; Martinez, R.; Hunter, T.; Sudarsanam, S. The protein kinase complement of the human genome. *Science* **2002**, *298* (5600), 1912–34.
(2) Blagoev, B.; Mann, M. Quantitative proteomics to study mitogen-activated protein kinases. *Methods* **2006**, *40* (3), 243–50.
(3) Blagoev, B.; Kratchmarova, I.; Ong, S. E.; Nielsen, M.; Foster, L. J.; Mann, M. A proteomics strategy to elucidate functional protein-protein interactions applied to EGF signaling. *Nat. Biotechnol.* **2003**, *21* (3), 315–8.
(4) Ong, S. E.; Blagoev, B.; Kratchmarova, I.; Kristensen, D. B.; Steen, H.; Pandey, A.; Mann, M. Stable isotope labeling by amino acids in cell culture, SILAC, as a simple and accurate approach to expression proteomics. *Mol. Cell. Proteomics* **2002**, *1* (5), 376–86.
(5) Kruger, M.; Kratchmarova, I.; Blagoev, B.; Tseng, Y. H.; Kahn, C. R.; Mann, M. Dissection of the insulin signaling pathway via quantitative phosphoproteomics. *Proc. Natl. Acad. Sci. U.S.A.* **2008**, *105* (7), 2451–6.
(6) Kratchmarova, I.; Blagoev, B.; Haack-Sorensen, M.; Kassem, M.; Mann, M. Mechanism of divergent growth factor effects in mesenchymal stem cell differentiation. *Science* **2005**, *308* (5727), 1472–7.
(7) Blagoev, B.; Ong, S. E.; Kratchmarova, I.; Mann, M. Temporal analysis of phosphotyrosine-dependent signaling networks by quantitative proteomics. *Nat. Biotechnol.* **2004**, *22* (9), 1139–45.
(8) Bose, R.; Molina, H.; Patterson, A. S.; Bitok, J. K.; Periaswamy, B.; Bader, J. S.; Pandey, A.; Cole, P. A. Phosphoproteomic analysis of Her2/neu signaling and inhibition. *Proc. Natl. Acad. Sci. U.S.A.* **2006**, *103* (26), 9773–8.
(9) Ponzetto, C.; Bardelli, A.; Zhen, Z.; Maina, F.; dalla Zonca, P.; Giordano, S.; Graziani, A.; Panayotou, G.; Comoglio, P. M. A multifunctional docking site mediates signaling and transformation by the hepatocyte growth factor/scatter factor receptor family. *Cell* **1994**, *77* (2), 261–71.
(10) Sachs, M.; Brohmann, H.; Zechner, D.; Muller, T.; Hulsken, J.; Walther, I.; Schaeper, U.; Birchmeier, C.; Birchmeier, W. Essential role of Gab1 for signaling by the c-Met receptor in vivo. *J. Cell Biol.* **2000**, *150* (6), 1375–84.
(11) Trusolino, L.; Comoglio, P. M. Scatter-factor and semaphorin receptors: cell signalling for invasive growth. *Nat. Rev. Cancer* **2002**, *2* (4), 289–300.
(12) Comoglio, P. M.; Trusolino, L. Invasive growth: from development to metastasis. *J. Clin. Invest.* **2002**, *109* (7), 857–62.
(13) Engelman, J. A.; Zejnullahu, K.; Mitsudomi, T.; Song, Y.; Hyland, C.; Park, J. O.; Lindeman, N.; Gale, C. M.; Zhao, X.; Christensen, J.; Kosaka, T.; Holmes, A. J.; Rogers, A. M.; Cappuzzo, F.; Mok, T.; Lee, C.; Johnson, B. E.; Cantley, L. C.; Janne, P. A. MET amplification leads to gefitinib resistance in lung cancer by activating ERBB3 signaling. *Science* **2007**, *316* (5827), 1039–43.
(14) Bean, J.; Brennan, C.; Shih, J. Y.; Riely, G.; Viale, A.; Wang, L.; Chitale, D.; Motoi, N.; Szoke, J.; Broderick, S.; Balak, M.; Chang, W. C.; Yu, C. J.; Gazdar, A.; Pass, H.; Rusch, V.; Gerald, W.; Huang, S. F.; Yang, P. C.; Miller, V.; Ladanyi, M.; Yang, C. H.; Pao, W. MET amplification occurs with or without T790M mutations in EGFR mutant lung tumors with acquired resistance to gefitinib or erlotinib. *Proc. Natl. Acad. Sci. U.S.A.* **2007**, *104* (52), 20932–7.
(15) Guo, A.; Villen, J.; Kornhauser, J.; Lee, K. A.; Stokes, M. P.; Rikova, K.; Possemato, A.; Nardone, J.; Innocenti, G.; Wetzel, R.; Wang, Y.; Macneill, J.; Mitchell, J.; Gygi, S. P.; Rush, J.; Polakiewicz, R. D.; Comb, M. J. Signaling networks assembled by oncogenic EGFR and c-Met. *Proc. Natl. Acad. Sci. U.S.A.* **2008**, *105* (2), 692–7.
(16) Shevchenko, A.; Wilm, M.; Vorm, O.; Mann, M. Mass spectrometric sequencing of proteins silver-stained polyacrylamide gels. *Anal. Chem.* **1996**, *68* (5), 850–8.
(17) Perkins, D. N.; Pappin, D. J.; Creasy, D. M.; Cottrell, J. S. Probability-based protein identification by searching sequence databases using mass spectrometry data. *Electrophoresis* **1999**, *20* (18), 3551–67.
(18) Cox, J.; Mann, M. MaxQuant enables high peptide identification rates, individualized p.p.b.-range mass accuracies and proteome-wide protein quantification. *Nat. Biotechnol.* **2008**, *26* (12), 1367–72.
(19) Zubarev, R.; Mann, M. On the proper use of mass accuracy in proteomics. *Mol. Cell. Proteomics* **2007**, *6* (3), 377–81.
(20) Olsen, J. V.; Blagoev, B.; Gnad, F.; Macek, B.; Kumar, C.; Mortensen, P.; Mann, M. Global, in vivo, and site-specific phosphorylation dynamics in signaling networks. *Cell* **2006**, *127* (3), 635–48.
(21) Zhang, Y.; Wolf-Yadlin, A.; Ross, P. L.; Pappin, D. J.; Rush, J.; Lauffenburger, D. A.; White, F. M. Time-resolved mass spectrometry of tyrosine phosphorylation sites in the epidermal growth factor receptor signaling network reveals dynamic modules. *Mol. Cell. Proteomics* **2005**, *4* (9), 1240–50.
(22) Stasyk, T.; Schiefermeier, N.; Skvortsov, S.; Zwierzina, H.; Peranen, J.; Bonn, G. K.; Huber, L. A. Identification of endosomal epidermal growth factor receptor signaling targets by functional organelle proteomics. *Mol. Cell. Proteomics* **2007**, *6* (5), 908–22.
(23) Chen, Y.; Low, T. Y.; Choong, L. Y.; Ray, R. S.; Tan, Y. L.; Toy, W.; Lin, Q.; Ang, B. K.; Wong, C. H.; Lim, S.; Li, B.; Hew, C. L.; Sze, N. S.; Druker, B. J.; Lim, Y. P. Phosphoproteomics identified Endofin, DCBLD2, and KIAA0582 as novel tyrosine phosphorylation targets of EGF signaling and Iressa in human cancer cells. *Proteomics* **2007**, *7* (14), 2384–97.
(24) Bublil, E. M.; Yarden, Y. The EGF receptor family: spearheading a merger of signaling and therapeutics. *Curr. Opin. Cell Biol.* **2007**, *19* (2), 124–34.
(25) Zhang, X.; Pickin, K. A.; Bose, R.; Jura, N.; Cole, P. A.; Kuriyan, J. Inhibition of the EGF receptor by binding of MIG6 to an activating kinase domain interface. *Nature* **2007**, *450* (7170), 741–4.
(26) Anastasi, S.; Fiorentino, L.; Fiorini, M.; Fraioli, R.; Sala, G.; Castellani, L.; Alema, S.; Alimandi, M.; Segatto, O. Feedback inhibition by RALT controls signal output by the ErbB network. *Oncogene* **2003**, *22* (27), 4221–34.
(27) Bohil, A. B.; Robertson, B. W.; Cheney, R. E. Myosin-X is a molecular motor that functions in filopodia formation. *Proc. Natl. Acad. Sci. U.S.A.* **2006**, *103* (33), 12411–6.
(28) Salatino, M.; Croci, D. O.; Bianco, G. A.; Ilarregui, J. M.; Toscano, M. A.; Rabinovich, G. A. Galectin-1 as a potential therapeutic target in autoimmune disorders and cancer. *Expert Opin. Biol. Ther.* **2008**, *8* (1), 45–57.
(29) Ho, E.; Irvine, T.; Vilk, G. J.; Lajoie, G.; Ravichandran, K. S.; D'Souza, S. J.; Dagnino, L. Integrin-linked Kinase Interactions with ELMO2Modulate Cell Polarity. *Mol. Biol. Cell* **2009**, *20*, 3033–43.
(30) Peacock, J. G.; Miller, A. L.; Bradley, W. D.; Rodriguez, O. C.; Webb, D. J.; Koleske, A. J. The Abl-related gene tyrosine kinase acts through p190RhoGAP to inhibit actomyosin contractility and regulate focal adhesion dynamics upon adhesion to fibronectin. *Mol. Biol. Cell* **2007**, *18* (10), 3860–72.
(31) Campbell, T. N.; Robbins, S. M. The Eph receptor/ephrin system: an emerging player in the invasion game. *Curr. Issues Mol. Biol.* **2008**, *10* (1−2), 61–6.
(32) Orian-Rousseau, V.; Chen, L.; Sleeman, J. P.; Herrlich, P.; Ponta, H. CD44 is required for two consecutive steps in HGF/c-Met signaling. *Genes Dev.* **2002**, *16* (23), 3074–86.
(33) Giordano, S.; Corso, S.; Conrotto, P.; Artigiani, S.; Gilestro, G.; Barberis, D.; Tamagnone, L.; Comoglio, P. M. The semaphorin 4D receptor controls invasive growth by coupling with Met. *Nat. Cell Biol.* **2002**, *4* (9), 720–4.
(34) Shannon, P.; Markiel, A.; Ozier, O.; Baliga, N. S.; Wang, J. T.; Ramage, D.; Amin, N.; Schwikowski, B.; Ideker, T. Cytoscape: a software environment for integrated models of biomolecular interaction networks. *Genome Res.* **2003**, *13* (11), 2498–504.
(35) Arcaro, A.; Zvelebil, M. J.; Wallasch, C.; Ullrich, A.; Waterfield, M. D.; Domin, J. Class II phosphoinositide 3-kinases are downstream targets of activated polypeptide growth factor receptors. *Mol. Cell. Biol.* **2000**, *20* (11), 3817–30.
(36) Falasca, M.; Hughes, W. E.; Dominguez, V.; Sala, G.; Fostira, F.; Fang, M. Q.; Cazzolli, R.; Shepherd, P. R.; James, D. E.; Maffucci, T. The role of phosphoinositide 3-kinase C2alpha in insulin signaling. *J. Biol. Chem.* **2007**, *282* (38), 28226–36.

(37) Maffucci, T.; Cooke, F. T.; Foster, F. M.; Traer, C. J.; Fry, M. J.; Falasca, M. Class II phosphoinositide 3-kinase defines a novel signaling pathway in cell migration. *J. Cell Biol.* **2005**, *169* (5), 789–99.
(38) Ramjaun, A. R.; Angers, A.; Legendre-Guillemin, V.; Tong, X. K.; McPherson, P. S. Endophilin regulates JNK activation through its interaction with the germinal center kinase-like kinase. *J. Biol. Chem.* **2001**, *276* (31), 28913–9.
(39) Findlay, G. M.; Yan, L.; Procter, J.; Mieulet, V.; Lamb, R. F. A MAP4 kinase related to Ste20 is a nutrient-sensitive regulator of mTOR signalling. *Biochem. J.* **2007**, *403* (1), 13–20.
(40) Rigden, D. J. The histidine phosphatase superfamily: structure and function. *Biochem. J.* **2008**, *409* (2), 333–48.
(41) Raguz, J.; Wagner, S.; Dikic, I.; Hoeller, D. Suppressor of T-cell receptor signalling 1 and 2 differentially regulate endocytosis and signalling of receptor tyrosine kinases. *FEBS Lett.* **2007**, *581* (24), 4767–72.
(42) Chan, G.; Kalaitzidis, D.; Neel, B. G. The tyrosine phosphatase Shp2 (PTPN11) in cancer. *Cancer Metastasis Rev.* **2008**, *27*, 179–92.
(43) Anitei, M.; Baust, T.; Czupalla, C.; Parshyna, I.; Bourel, L.; Thiele, C.; Krause, E.; Hoflack, B., Protein Networks Supporting AP-3 Function in Targeting Lysosomal Membrane Proteins. *Mol. Biol. Cell* **2008**, *19*, 1942–51.
(44) Spiliotis, E. T.; Hunt, S. J.; Hu, Q.; Kinoshita, M.; Nelson, W. J. Epithelial polarity requires septin coupling of vesicle transport to polyglutamylated microtubules. *J. Cell Biol.* **2008**, *180* (2), 295–303.
(45) Hunter, T. The age of crosstalk: phosphorylation, ubiquitination, and beyond. *Mol. Cell* **2007**, *28* (5), 730–8.
(46) Levkowitz, G.; Waterman, H.; Zamir, E.; Kam, Z.; Oved, S.; Langdon, W. Y.; Beguinot, L.; Geiger, B.; Yarden, Y. c-Cbl/Sli-1 regulates endocytic sorting and ubiquitination of the epidermal growth factor receptor. *Genes Dev.* **1998**, *12*, 3663–3674.
(47) Peschard, P.; Fournier, T. M.; Lamorte, L.; Naujokas, M. A.; Band, H.; Langdon, W. Y.; Park, M. Mutation of the c-Cbl TKB domain binding site on the Met receptor tyrosine kinase converts it into a transforming protein. *Mol. Cell* **2001**, *8*, 995–1004.
(48) Masuda-Robens, J. M.; Kutney, S. N.; Qi, H.; Chou, M. M. The TRE17 oncogene encodes a component of a novel effector pathway for Rho GTPases Cdc42 and Rac1 and stimulates actin remodeling. *Mol. Cell. Biol.* **2003**, *23* (6), 2151–61.
(49) Martinu, L.; Masuda-Robens, J. M.; Robertson, S. E.; Santy, L. C.; Casanova, J. E.; Chou, M. M. The TBC (Tre-2/Bub2/Cdc16) domain protein TRE17 regulates plasma membrane-endosomal trafficking through activation of Arf6. *Mol. Cell. Biol.* **2004**, *24* (22), 9752–62.
(50) Chen, H.; Polo, S.; Di Fiore, P. P.; De Camilli, P. V. Rapid Ca2+-dependent decrease of protein ubiquitination at synapses. *Proc. Natl. Acad. Sci. U.S.A.* **2003**, *100* (25), 14908–13.
(51) Al-Hakim, A. K.; Zagorska, A.; Chapman, L.; Deak, M.; Peggie, M.; Alessi, D. R. Control of AMPK-related kinases by USP9X and atypical Lys29/Lys33-linked polyubiquitin chains. *Biochem. J.* **2008**, *411*, 249–60.

PR100145W